Supporting Information for

Tuning the Electronic Effects of a Redox-Active Triamido Ligand in d^0 Tantalum Complexes

Rui F. Munhá , Ryan A. Zarkesh and Alan F. Heyduk*

Department of Chemistry, University of California Irvine, California, 92697-2025 United States.
E-mail: aheyduk@uci.edu

Page

Figure S15. ORTEP diagram for $^{OMe,iPr}(NNN^{q})TaCl_2$ ($NPh^{4\text{-}tBu}$) (**7a**). Thermal ellipsoids are drawn at 50% probability. Co-crystallized solvent molecules and hydrogen atoms have been omitted for clarity.

Spectroscopic Data $^{X,R}(NNN^{sq})TaCl_3$

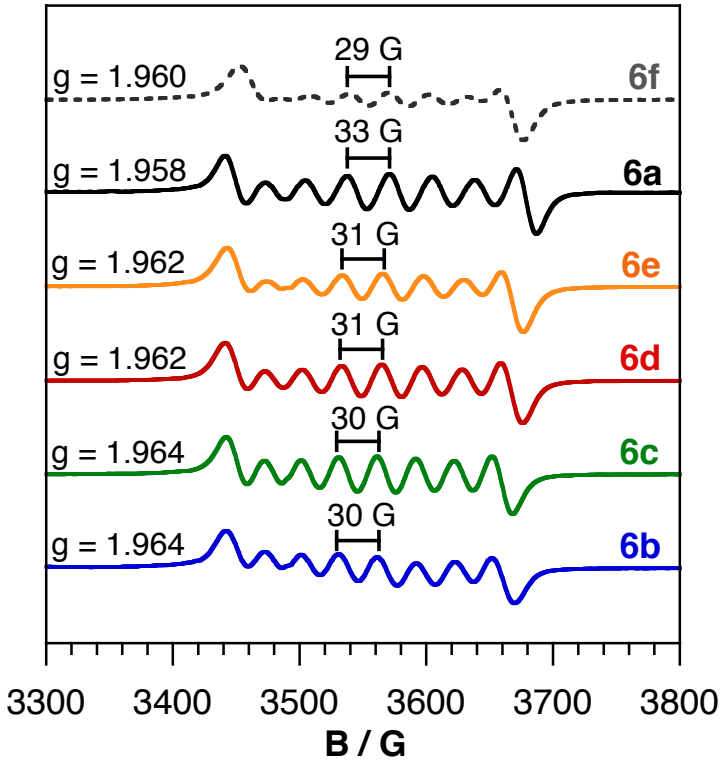

Figure S1. EPR spectra of $^{X,R}(NNN^{sq})TaCl_3$ (**6a-f**) collected at 298 K in C_7H_8 .$^{OMe,iPr}(NNN^{sq})TaCl_3$ (**6a**, *black*), $^{F,iPr}(NNN^{sq})TaCl_3$ (**6b**, *blue*), $^{H,iPr}(NNN^{sq})TaCl_3$ (**6c**, *green*), $^{Me,iPr}(NNN^{sq})TaCl_3$ (**6d**, *red*), $^{tBu,iPr}(NNN^{sq})TaCl_3$ (**6e**, *orange*), $^{OMe,DMP}(NNN^{sq})TaCl_3$ (**6f**, *black, dotted line*).

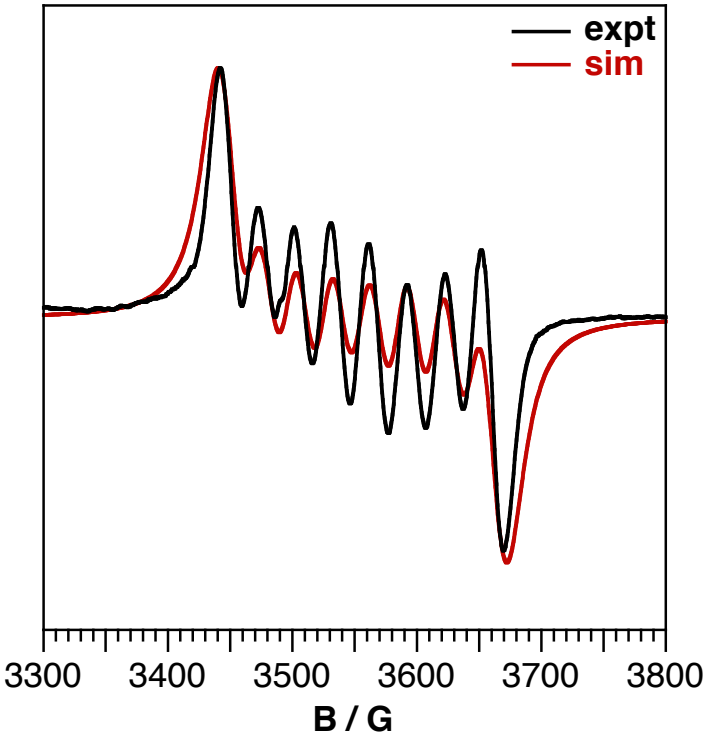

Figure S2. EPR spectrum of $^{F,iPr}(NNN^{sq})TaCl_3$ (**6b**) collected at 298 K in C_7H_8 (**expt**) and the corresponding simulated spectrum (**sim**).

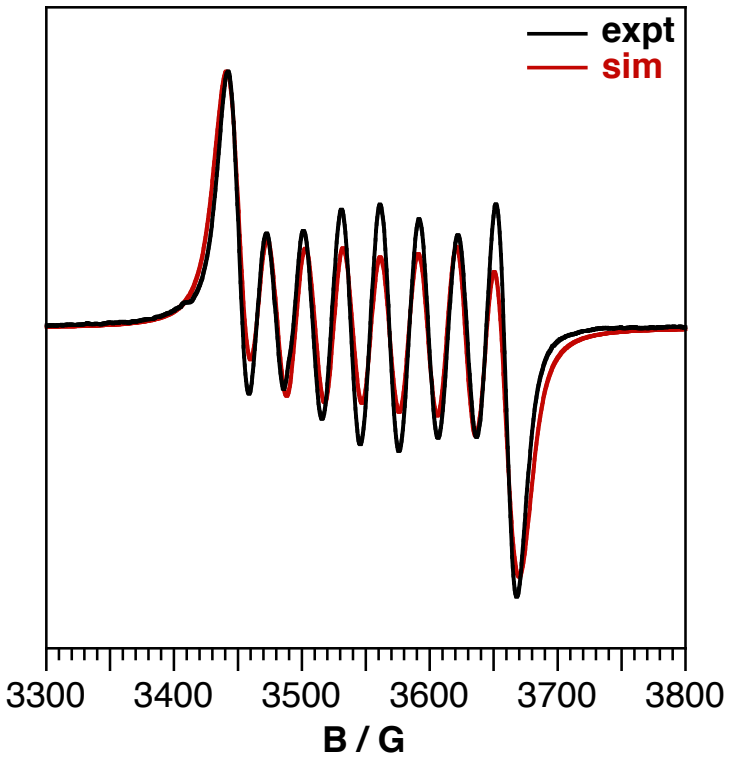

Figure S3. EPR spectrum of $^{H,iPr}(NNN^{sq})TaCl_3$ (**6c**) collected at 298 K in C_7H_8 (**expt**) and the corresponding simulated spectrum (**sim**).

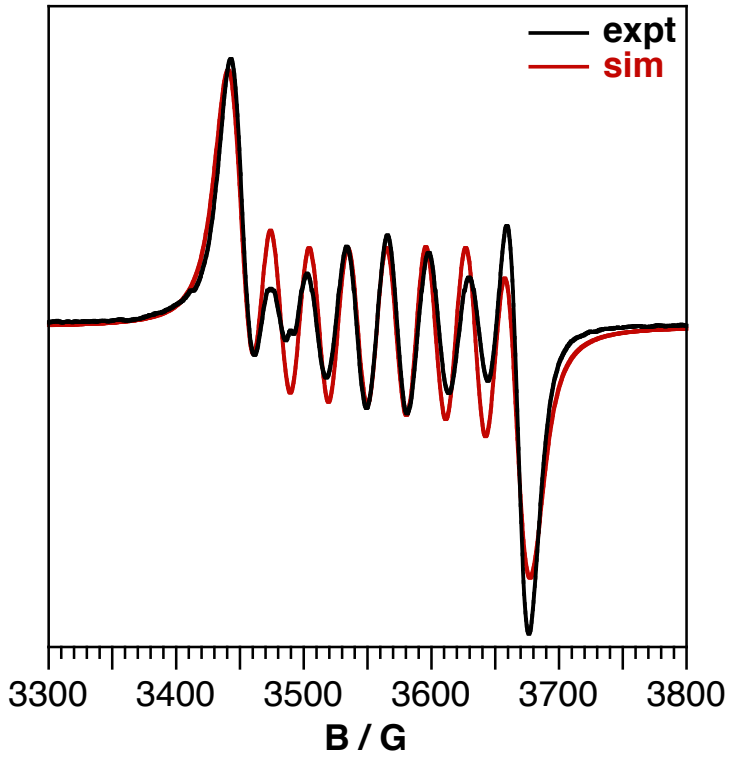

Figure S4. EPR spectrum of $^{tBu,iPr}(NNN^{sq})TaCl_3$ (**6e**) collected at 298 K in C_7H_8 (**expt**) and the corresponding simulated spectrum (**sim**).

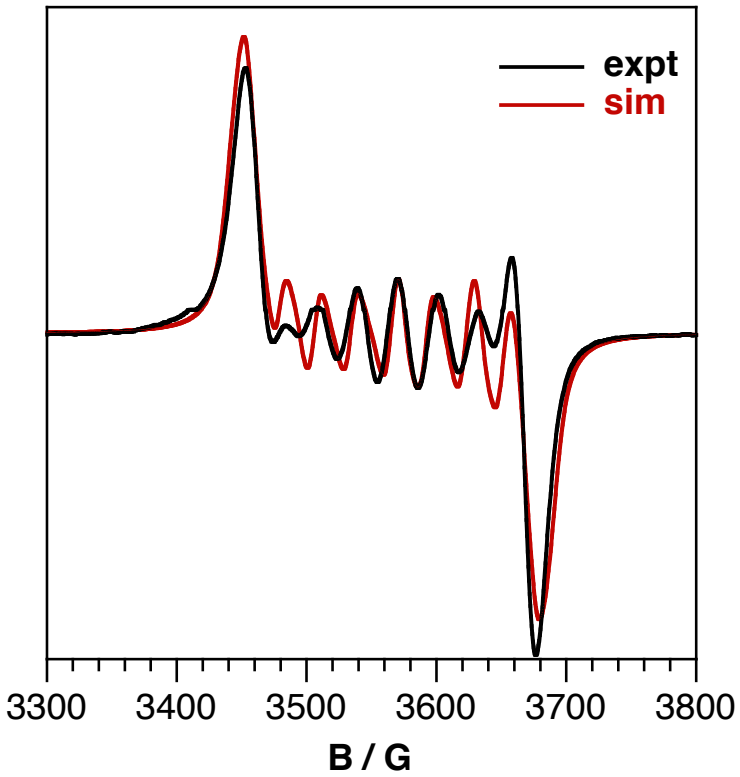

Figure S5. EPR spectrum of $^{OMe,DMP}(NNN^{sq})TaCl_3$ (**6f**) collected at 298 K in C_7H_8 (**expt**) and the corresponding simulated spectrum (**sim**).

Spectroscopic Data $^{X,R}(NNN^{q})TaCl_2(NPh^{4\text{-}R'})$

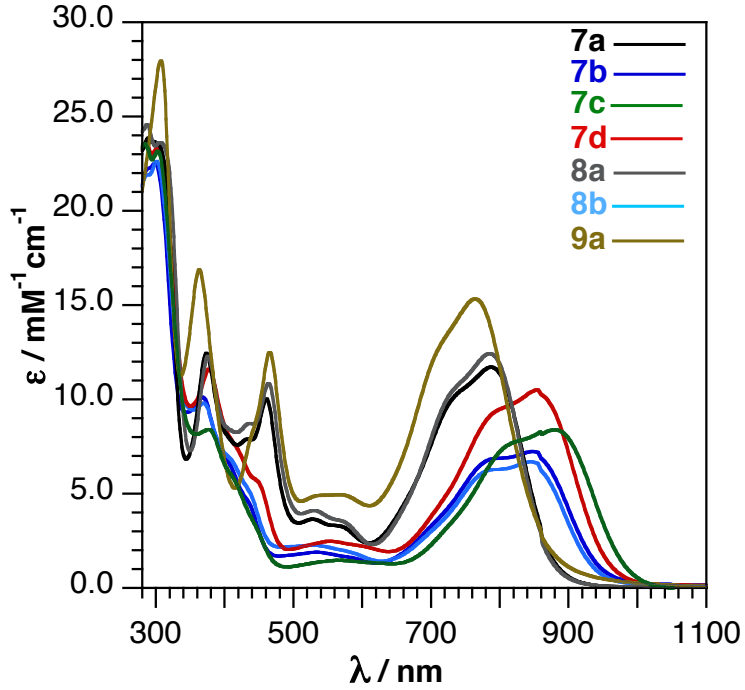

Figure S6. Uv-vis-NIR spectra of $^{X,R}(NNN^{q})TaCl_2(NPh^{4\text{-}R'})$ (**7a-d, 8a-b, 9a**) collected at 298 K in THF. $^{OMe,iPr}(NNN^{q})TaCl_2(NPh^{4\text{-}tBu})$ (**7a**, *black*), $^{F,iPr}(NNN^{q})TaCl_2(NPh^{4\text{-}tBu})$ (**7b**, *blue*), $^{H,iPr}(NNN^{q})TaCl_2(NPh^{4\text{-}tBu})$ (**7c**, *green*), $^{Me,iPr}(NNN^{q})TaCl_2(NPh^{4\text{-}tBu})$ (**7d**, *red*), $^{OMe,iPr}(NNN^{q})TaCl_2(NPh^{4\text{-}CF3})$ (**8a**, *grey*), $^{F,iPr}(NNN^{q})TaCl_2(NPh^{4\text{-}CF3})$ (**8b**, *light blue*), $^{OMe,DMP}(NNN^{q})TaCl_2(NPh^{4\text{-}Me})$ (**9a**, *brown, dotted line*).

^{1}H NMR and ^{19}F NMR spectra of the diamagnetic compounds 7b and 8b. ^{13}C NMR spectrum of 7b.

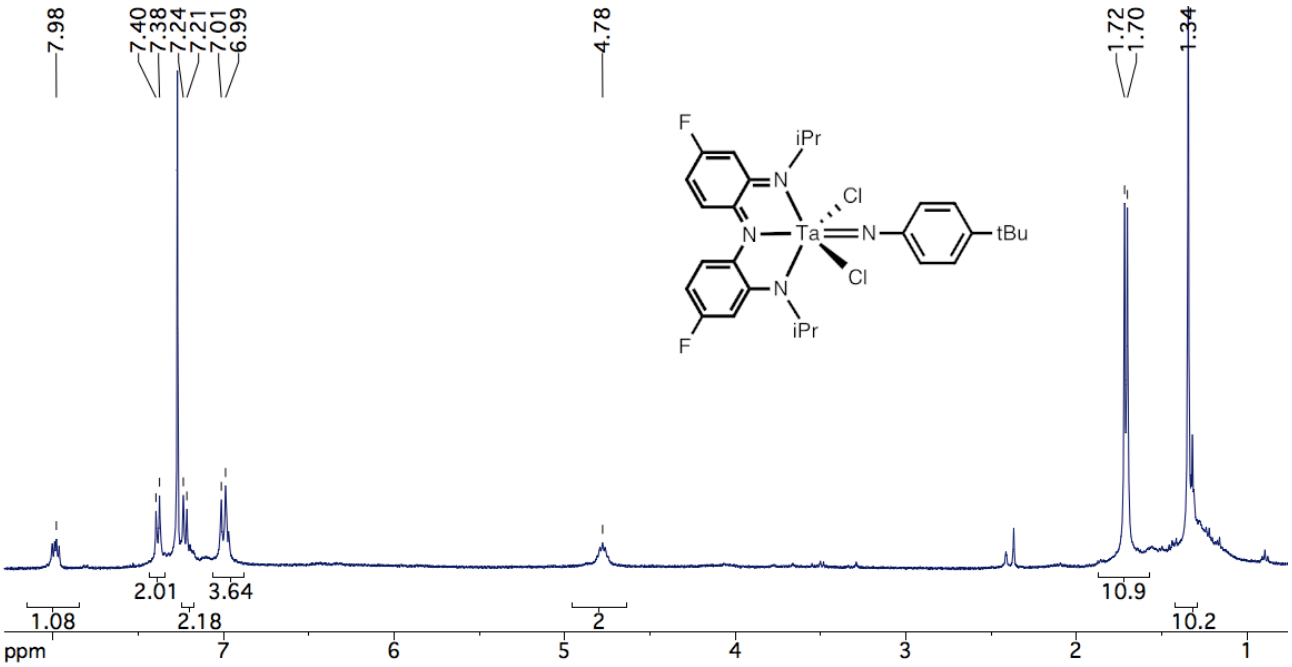

Figure S7. ^{1}H NMR spectrum of ^{F,iPr}(NNN^{q})TaCl$_2$(NPh$^{4\text{-}tBu}$) (**7b**) in $CDCl_3$ at 298K.

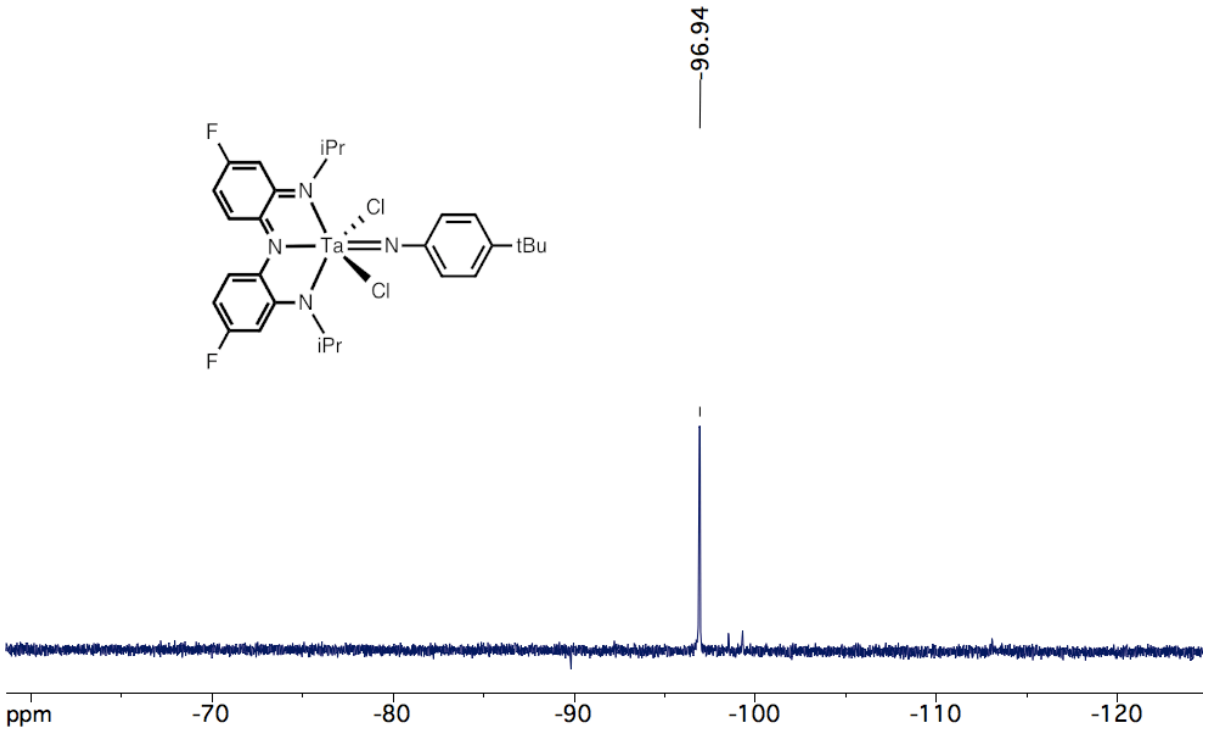

Figure S8. ^{19}F NMR spectrum of ^{F,iPr}(NNN^{q})TaCl$_2$(NPh$^{4\text{-}tBu}$) (**7b**) in $CDCl_3$ at 298K.

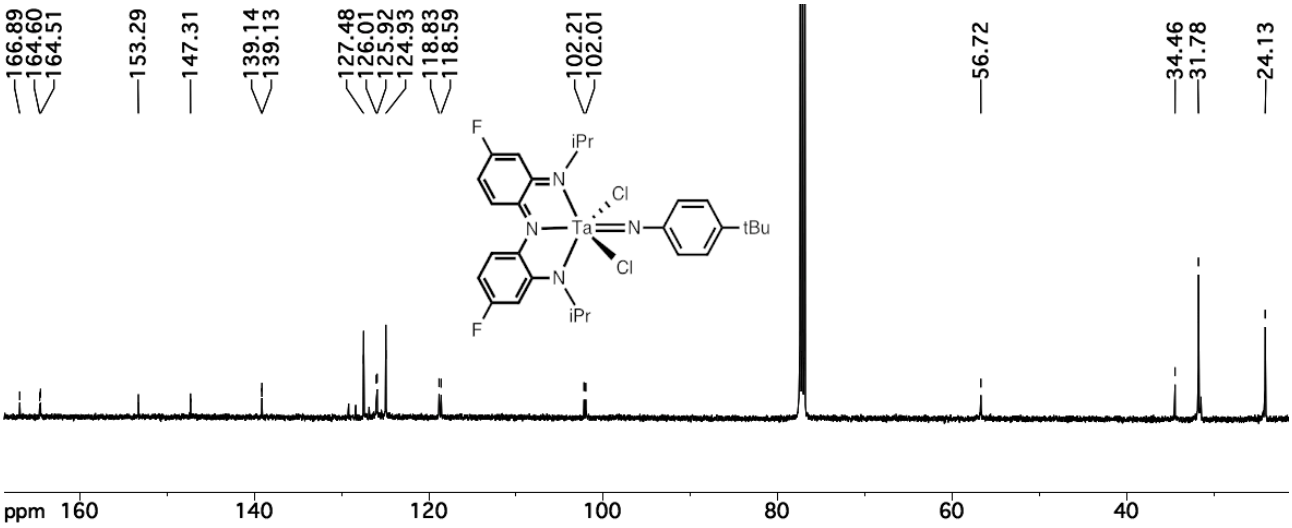

Figure S9. ^{13}C NMR spectrum of $^{F,iPr}(NNN^{q})TaCl_2(NPh^{4\text{-}tBu})$ (**7b**) in $CDCl_3$ at 298K.

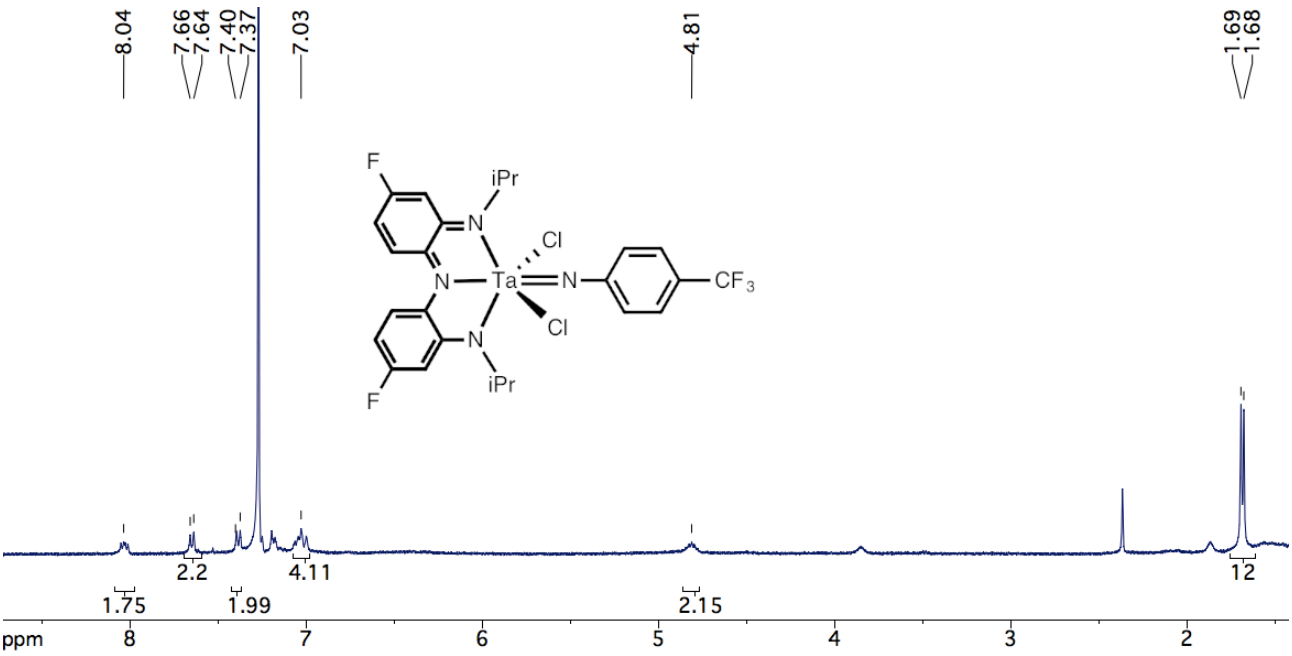

Figure S10. ^{1}H NMR spectrum of $^{F,iPr}(NNN^{q})TaCl_2(NPh^{4\text{-}CF3})$ (**8b**) in $CDCl_3$ at 298K.

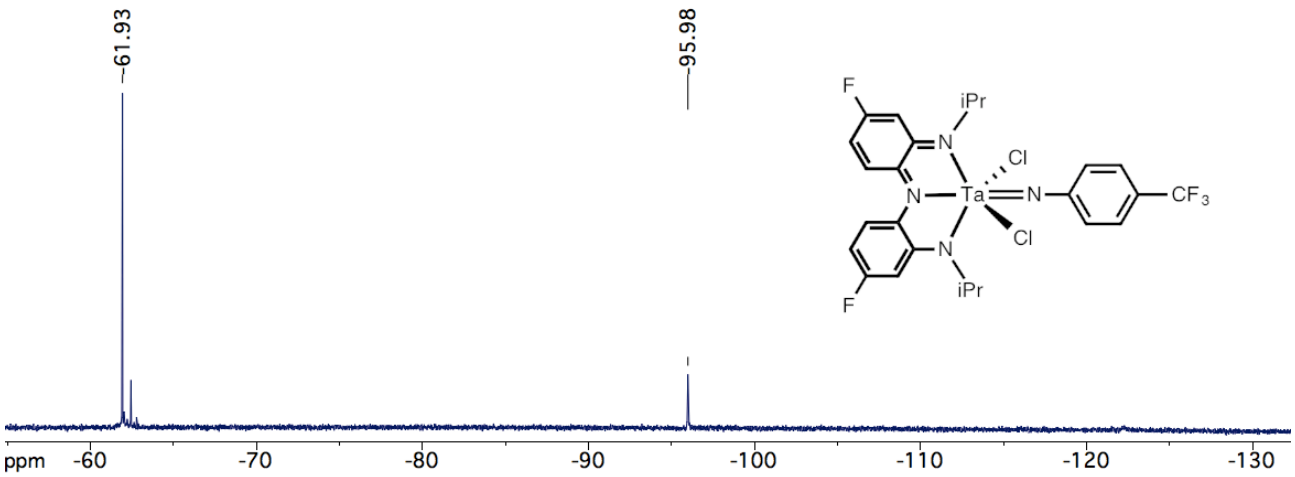

Figure S11. ^{19}F NMR spectrum of $^{F,iPr}(NNN^{q})TaCl_2(NPh^{4\text{-}CF3})$ (**8b**) in $CDCl_3$ at 298K.

Table S1. X-ray diffraction data for the tantalum complexes of the general formula $^{X,R}(NNN^{cat})TaCl_2$ (**3b-f**).

	$^{F,iPr}(NNN^{cat})TaCl_2$ **3b, (C_7H_8)$_{0.5}$**	$^{H,iPr}(NNN^{cat})TaCl_2$ **3c**	$^{Me,iPr}(NNN^{cat})TaCl_2$ **3d, (C_6H_6)**	$^{tBu,iPr}(NNN^{cat})TaCl_2$ **3e**	$^{OMe,DMP}(NNN^{cat})TaCl_2$ **3f•(OEt_2)**
Empirical formula	$C_{18}H_{20}N_3F_2Cl_2Ta$, $(C_7H_8)_{0.5}$	$C_{18}H_{22}N_3Cl_2Ta$	$C_{20}H_{26}N_3Cl_2Ta$, (C_6H_6)	$C_{26}H_{38}N_3Cl_2Ta$	$C_{34}H_{10}N_3O_3Cl_2Ta$
Formula weight	614.29	532.24	638.39	644.44	790.54
Crystal system	*Triclinic*	*Monoclinic*	*Orthorhombic*	*Monoclinic*	*Orthorhombic*
Space group	*P*-1	$P2_1/c$	*P*nna	*C*2/c	*P*bca
T (K)	88(2)	88(2)	143(2)	88(2)	143(2)
a / Å	7.4773(4)	11.2405(15)	9.8131(6)	22.2922(10)	15.8487(8)
b / Å	11.8614(6)	22.330(3)	10.6877(6)	19.3663(9)	15.9239(8)
c / Å	12.6098(7)	14.758(2)	23.9902(14)	12.6188(6)	25.9100(14)
α / °	76.4926(5)	90	90	90	90
β / °	81.4203(6)	94.6604(16)	90	95.5609(5)	90
γ / °	87.9507(6)	90	90	90	90
V (Å^3)	1075.27(10)	3692.2(9)	2516.1(3)	5422.1(4)	6539.0(6)
Z	2	8	4	8	8
Reflections collected	13030	43506	26584	32484	67516
data/restraints/parameters	5156 / 0 / 302	9122 / 0 / 441	2789 / 0 / 146	6742 / 0 / 299	6694 / 0 / 396
R1 [$I > 2\sigma(I)$][a]	0.0144	0.0271	0.0205	0.0146	0.0263
wR2 (all data)[a]	0.0358	0.0576	0.0529	0.0348	0.0584
GOF[a]	1.056	1.096	1.123	1.036	1.018

[a] $R1 = \Sigma||F_o| - |F_c||/\Sigma|F_o|$; $wR2 = [\Sigma[w(F_o^2 - F_c^2)^2]/\Sigma[w(F_o^2)^2]]^{1/2}$; $GOF = [\Sigma w(|F_o| - |F_c|)^2/(n - m)]^{1/2}$

Table S2. X-ray diffraction data for $^{OMe,DMP}(NNN^{sq})TaCl_3$ (**6f**), $^{OMe,iPr}(NNN^{q})TaCl_2(NPh^{4\text{-}tBu})$ (**7a**), $^{Me,iPr}(NNN^{q})TaCl_2(NPh^{4\text{-}tBu})$ (**7d**).

	$^{OMe,DMP}(NNN^{sq})TaCl_3$ **6f, (C_7H_8)**	$^{OMe,iPr}(NNN^{q})TaCl_2(NPh^{4\text{-}tBu})$ **7a**	$^{Me,iPr}(NNN^{q})TaCl_2(NPh^{4\text{-}tBu})$ **7d**
Empirical formula	$C_{30}H_{30}N_3O_2Cl_3Ta$, (C_7H_8)	$C_{30}H_{39}N_4O_2Cl_2Ta$, $(C_7H_8)_{3.5}$	$C_{30}H_{39}N_4O_2Cl_2Ta$, (C_7H_8)
Formula weight	844.00	1057.94	799.63
Crystal system	*Monoclinic*	*Triclinic*	*Triclinic*
Space group	$P2_1/n$	P-1	P-1
T (K)	143(2)	143(2)	143(2)
a / Å	7.9327(5)	10.9766(7)	9.5476(7)
b / Å	22.8472(15)	13.0697(9)	12.9593(9)
c / Å	19.0689(13)	19.1327(13)	14.6178(10)
α / ^{o}	90	108.9610(10)	82.2726(8)
β / ^{o}	92.0210(10)	101.4700(10)	84.9424(8)
γ / ^{o}	90	91.2710(10)	81.0999(8)
V (Å^3)	3453.9(4)	2532.8(3)	1766.5(2)
Z	4	2	2
Reflections collected	29030	25586	20136
data/restraints/parameters	7991 / 0 / 415	9282 / 0 / 574	8026 / 0 / 407
R1 [$I > 2\sigma(I)$][a]	0.0362	0.0259	0.0240
wR2 (all data)[a]	0.0876	0.0648	0.0593
GOF[a]	1.074	1.047	1.066

[a] $R1 = \Sigma||F_o| - |F_c||/\Sigma|F_o|$; $wR2 = [\Sigma[w(F_o^2 - F_c^2)^2]/\Sigma[w(F_o^2)^2]]^{1/2}$; $GOF = [\Sigma w(|F_o| - |F_c|)^2/(n - m)]^{1/2}$

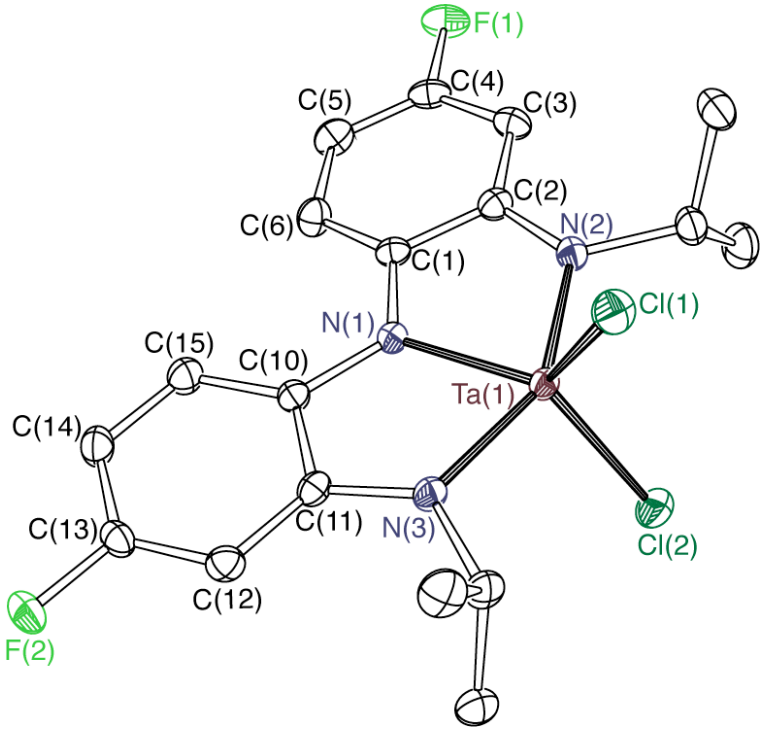

Figure S12. ORTEP diagram for $^{F,iPr}(NNN^{cat})TaCl_2$ (**3b**). Thermal ellipsoids are drawn at 50% probability. Co-crystallized solvent molecules and hydrogen atoms have been omitted for clarity.

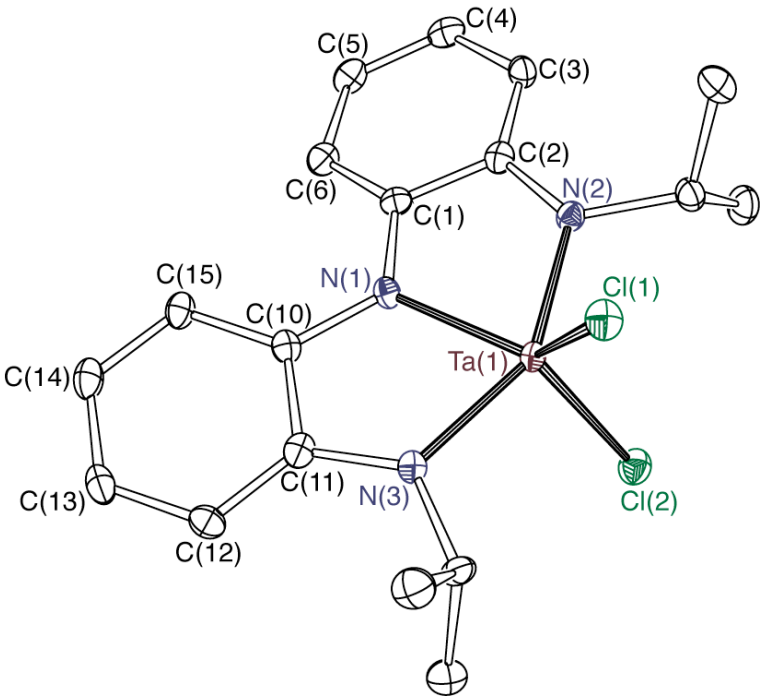

Figure S13. ORTEP diagram for $^{H,iPr}(NNN^{cat})TaCl_2$ (**3c**). Thermal ellipsoids are drawn at 50% probability. One molecule of the asymmetric unit shown, where hydrogen atoms have been omitted for clarity.

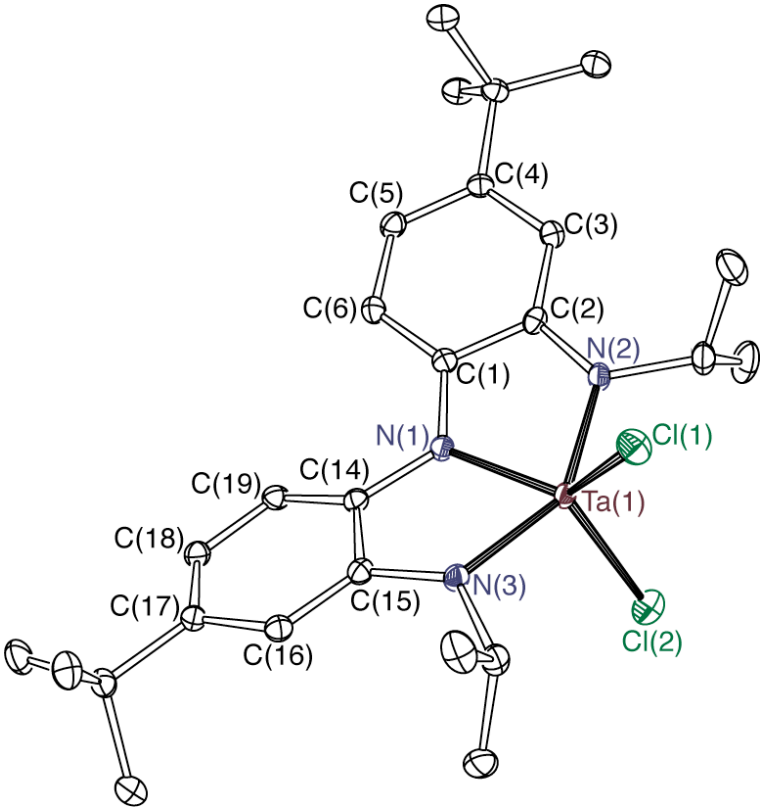

Figure S14. ORTEP diagram for $^{tBu,iPr}(NNN^{cat})TaCl_2$ (**3e**). Thermal ellipsoids are drawn at 50% probability. Hydrogen atoms have been omitted for clarity.

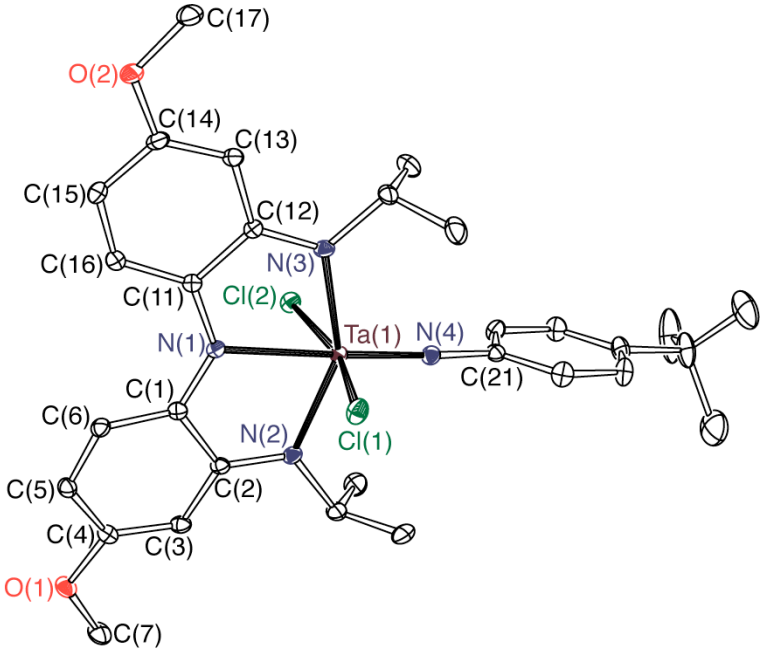

Figure S15. ORTEP diagram for $^{OMe,iPr}(NNN^{q})TaCl_2$ ($NPh^{4\text{-}tBu}$) (**7a**). Thermal ellipsoids are drawn at 50% probability. Co-crystallized solvent molecules and hydrogen atoms have been omitted for clarity.